Letters

A Rotation-Free Wireless Power Transfer System With Stable Output Power and Efficiency for Autonomous Underwater Vehicles

Zhengchao Yan, *Student Member, IEEE*, Baowei Song, Yiming Zhang, *Member, IEEE*, Kehan Zhang, Zhaoyong Mao, and Yuli Hu

***Abstract*—This letter proposes a rotation-free wireless power transfer system based on a new coil structure to achieve stable output power and efficiency against rotational misalignments for charging autonomous underwater vehicles. The new coil structure has two decoupled receivers composed of two reversely wound receiver coils and the magnetic flux directions of the two receivers are perpendicular to each other, guaranteeing a relatively constant total mutual inductance and a decoupled characteristic under rotational misalignments. The proposed coil structure is verified via finite element analysis based on ANSYS Maxwell. A rotation-free *LCC–LCC* compensated WPT prototype is built and the experimental results verify the theoretical analysis and simulations. The system can deliver 664 W with a dc–dc efficiency of 92.26% under the best case and 485 W with a 92.10% dc–dc efficiency under the worst case.**

***Index Terms*—Autonomous underwater vehicles (AUVs), decoupled, rotation-free, wireless power transfer (WPT).**

I. Introduction

WIRELESS power transfer (WPT) technology can be applied in numerous situations [1], [2], such as autonomous underwater vehicles (AUVs) [3], [4]. The concealment and utilization rate of the AUV can be significantly improved by using a seafloor base station to supply power wirelessly to the AUV. Feezor *et al*. [3] developed a wireless charging system, which could transfer 200 W power and signals for the AUV. Li *et al*. [4] designed an underwater WPT system and

Manuscript received July 12, 2018; revised August 19, 2018; accepted September 15, 2018. Date of publication September 18, 2018; date of current version March 29, 2019. This work was supported in part by the Natural Science Basic Research Plan in Shaanxi Province of China under Grants 2018JM5033 and 2018JQ5042 and in part by the National Natural Science Foundation of China under Grant 51809214. *(Corresponding author: Kehan Zhang.)*

Z. Yan is with the School of Marine Science and Technology, Northwestern Polytechnical University, Xi'an 710072, China (e-mail:

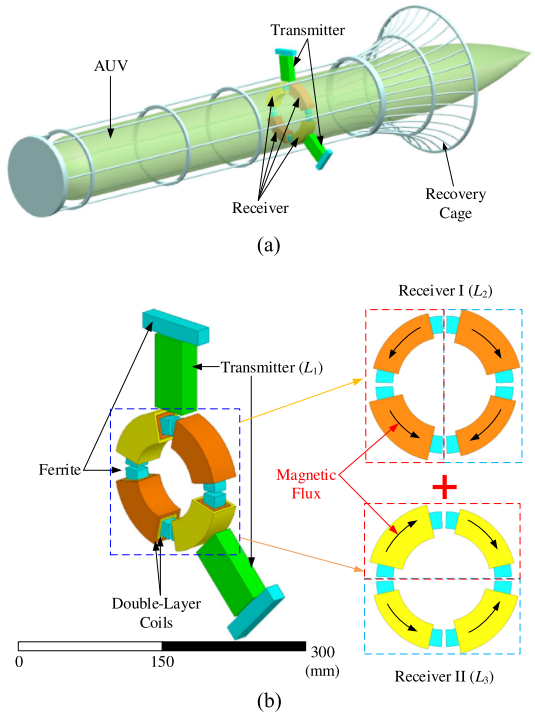

Fig. 1. (a) General overview of the WPT system for AUVs. (b) Proposed rotation-free coil structure.

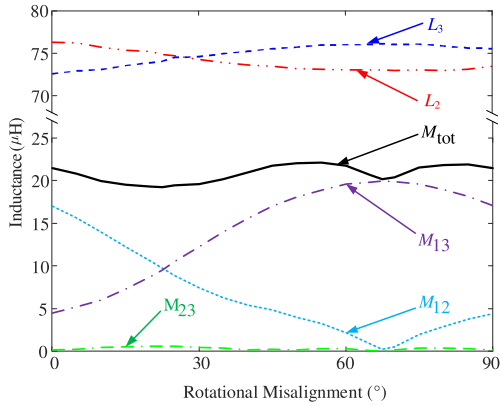

Fig. 2. Simulated self-inductances and mutual inductances.

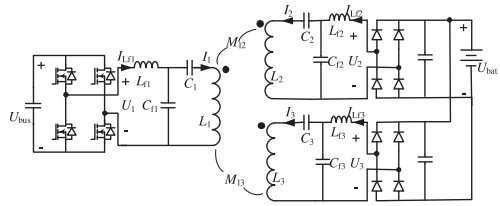

Fig. 3. Circuit topology.

wireless charging process can be performed for the AUV. The proposed new coil structure is shown in Fig. 1(b). It consists of one transmitter (L_1) with two green rectangular windings and two double-layer receivers, namely Receiver I (L_2) with four orange circular windings and Receiver II (L_3) with four yellow circular windings. These eight windings are wound on the circular ferrites in a double-layer way. For the purpose of symmetry, each receiver is composed of alternate inner and outer windings, with two reversely wound directions, and the magnetic flux directions of the two receivers are perpendicular to each other, guaranteeing a relatively constant total mutual inductance and a decoupled characteristic against rotational misalignments.

The self-inductances of Receiver I (L_2) and Receiver II (L_3), the mutual inductances between the transmitter and Receivers I and II (M_{12} and M_{13}), and the mutual inductance between the receivers (M_{23}) varying with the rotational misalignments simulated in ANSYS Maxwell are shown in Fig. 2. L_2 and L_3 remain relatively stable and identical due to the alternate inner and outer coil structure. M_{23} is small enough to be neglected. The total mutual inductance between the transmitter and the receivers M_{tot} presents a relatively stable trend, which can be expressed as follows:

$$M_{\mathrm{tot}} = |M_{12}| + |M_{13}|. \tag{1}$$

III. Circuit Analysis

The circuit topology for the proposed WPT system is depicted in Fig. 3, where the *LCC–LCC* topology is adopted to keep the coil currents constant against rotational misalignments. The double-sided *LCC* topology has a constant-current output, which enables the parallel connection of the two rectifiers on the receiver side. On the transmitter side, L_1 is the transmission inductance, C_1 is the series compensation capacitance, C_{f1} is the parallel compensation capacitance, L_{f1} is the compensation inductance, U_{bus} is the inverter dc voltage, and U_1 is the inverter ac voltage. L_2 (L_3), C_2 (C_3), C_{f2} (C_{f3}), L_{f2} (L_{f3}), U_{bat}, and U_2 (U_3) are their counterparts of Receiver I (II).

At resonance, we have

$$j\omega_0 L_{\mathrm{f}i} + \frac{1}{j\omega_0 C_{\mathrm{f}i}} = 0, \quad j\omega_0 L_i + \frac{1}{j\omega_0 C_i} + \frac{1}{j\omega_0 C_{\mathrm{f}i}} = 0, \quad i = 1, 2, 3 \tag{2}$$

where ω_0 is the resonant angular frequency. With the Fourier decomposition, U_1, U_2, and U_3 can be obtained as follows:

$$U_1 = \frac{2\sqrt{2}}{\pi} U_{\mathrm{bus}}, \quad U_2 = \frac{2\sqrt{2}}{\pi} U_{\mathrm{bat}}, \quad U_3 = \frac{2\sqrt{2}}{\pi} U_{\mathrm{bat}}. \tag{3}$$

The currents can be obtained as follows:

$$\begin{cases} I_{\mathrm{Lf1}} = \frac{1}{\omega_0 L_{\mathrm{f1}}} \left(\frac{M_{12} U_2}{L_{\mathrm{f2}}} + \frac{M_{13} U_3}{L_{\mathrm{f3}}} \right), \\ I_{\mathrm{Lf2}} = \frac{M_{12} U_1}{\omega_0 L_{\mathrm{f1}} L_{\mathrm{f2}}}, I_{\mathrm{Lf3}} = \frac{M_{13} U_1}{\omega_0 L_{\mathrm{f1}} L_{\mathrm{f3}}} \\ I_1 = \frac{U_1}{\omega_0 L_{\mathrm{f1}}}, \quad I_2 = \frac{U_2}{\omega_0 L_{\mathrm{f2}}}, \quad I_3 = \frac{U_3}{\omega_0 L_{\mathrm{f3}}}. \end{cases} \tag{4}$$

The receivers are identical: $L_1 = L_2$ and $L_{\mathrm{f2}} = L_{\mathrm{f3}}$. The output power can be calculated as follows:

$$P_{\mathrm{out}} = U_2 I_{\mathrm{f2}} + U_3 I_{\mathrm{f3}} = \frac{8 U_{\mathrm{bus}} U_{\mathrm{bat}} M_{\mathrm{tot}}}{\pi^2 \omega_0 L_{\mathrm{f1}} L_{\mathrm{f2}}}. \tag{5}$$

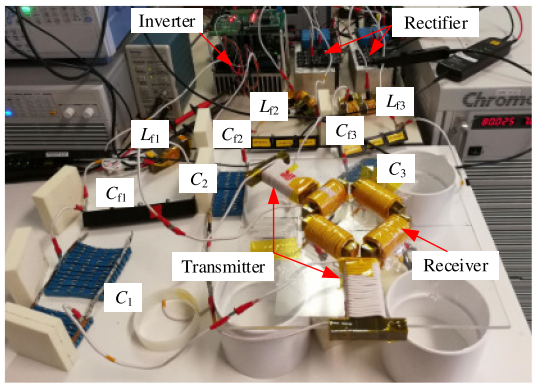

Fig. 4. Experimental prototype.

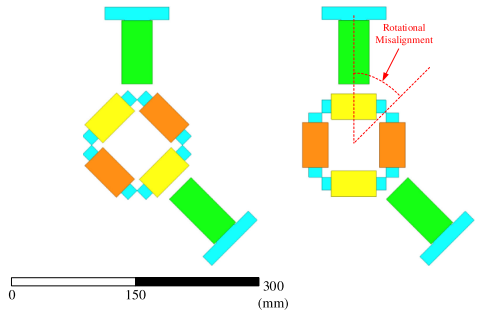

Fig. 5. Simulation model of the practical coil structure.

It can be seen that P_{out} is proportional to U_{bus}, U_{bat}, and M_{tot}. The transfer efficiency η can be expressed as

$$\eta = \frac{P_{\text{out}}}{P_{\text{out}} + I_1^2 R_1 + I_2^2 R_2 + I_3^2 R_3 + I_{\text{Lf1}}^2 R_{\text{Lf1}} + I_{\text{Lf2}}^2 R_{\text{Lf2}} + I_{\text{Lf3}}^2 R_{\text{Lf3}}} \tag{6}$$

where R_1, R_2, and R_3 denote the equivalent resistances of the transmitter and receivers; R_{Lf1}, R_{Lf2}, and R_{Lf3} represent the equivalent resistances of the compensation coils.

IV. Experimental Verification

An experimental prototype based on the proposed rotation-free coil structure is implemented, as shown in Fig. 4. The arc cores for the receivers are unavailable, so the ferrite bars are adopted as a replacement in the prototype. The simulated model of the practical coil structure is shown in Fig. 5. The rotational misalignments vary from 0° to 90° both in the simulations, and the experiments for 90° is the rotational period. The system specifications and the circuit parameters at the best case are tabulated in Table I.

Fig. 6 shows the simulated and measured total mutual inductances varying with the rotational misalignments, which indicates that the total mutual inductance remains approximately identical during rotational misalignments. The total mutual inductance is maximized at 0° and minimized at 22.5°. The discrepancies between the measurements and the simulations may be caused by the parameter mismatch.

The dc–dc efficiency and the output power varying with the rotational misalignments are shown in Fig. 7. The efficiency and the output power remain relatively stable against rotational misalignments. The system can deliver 664 W with a dc–dc efficiency of 92.26% under the best case of 0° and 485 W with a 92.10% dc–dc efficiency under the worst case of 22.5°.

TABLE I
System Specifications and Circuit Parameters

U_{bus}	U_{bat}	L_1	L_2	L_3
160 V	80 V	108.3 μH	74.3 μH	74.7 μH
M_{12}	M_{13}	C_{f1}	C_{f2}	C_{f3}
15.1 μH	3.1 μH	25.3 nF	34.2 nF	34.5 nF
C_1	C_2	C_3	f_0	
4.2 nF	6.5 nF	6.1 nF	252.6 kHz	

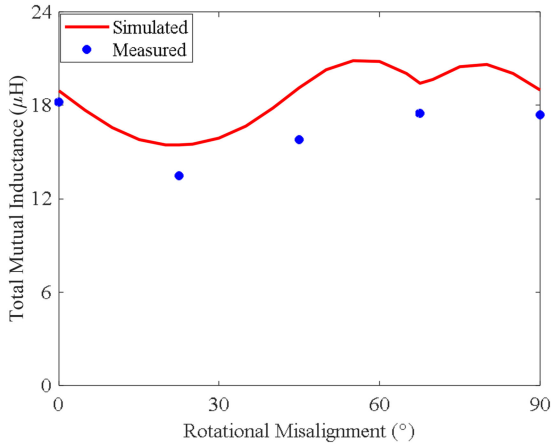

Fig. 6. Simulated and measured total mutual inductances.

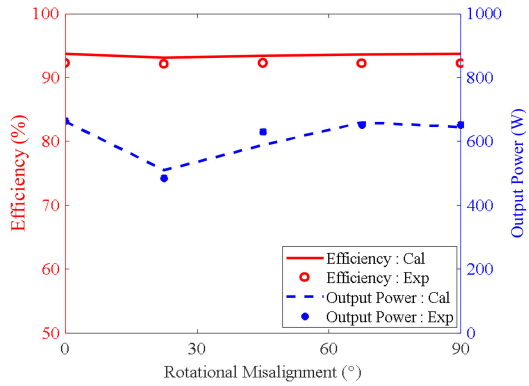

Fig. 7. DC–DC efficiency and output power versus rotational misalignments.

V. Conclusion

A rotation-free WPT system based on a new coil structure for charging the AUVs has been proposed. The two receivers are decoupled and the total mutual inductance remains relatively stable. Therefore, constant output power and efficiency are achieved against rotational misalignments. A rotation-free WPT prototype has been built and the experimental results have verified the theoretical analysis and simulations. The system can deliver 664 W with a dc–dc efficiency of 92.26% under the best case of 0° and 485 W with a 92.10% dc–dc efficiency under the worst case of 22.5°.

References

[1] S. Li and C. C. Mi, "Wireless power transfer for electric vehicle applications," *IEEE J. Emerg. Sel. Topics Power Electron.*, vol. 3, no. 1, pp. 4–17, Mar. 2015.

[2] Y. Zhang, T. Kan, Z. Yan, Y. Mao, Z. Wu, and C. Mi, "Modeling and analysis of series-none compensation for wireless power transfer systems with a strong coupling," *IEEE Trans. Power Electron.*, to be published, doi: 10.1109/TPEL.2018.2835307.

[3] M. D. Feezor, F. Y. Sorrell, and P. R. Blankinship, "An interface system for autonomous undersea vehicles," *IEEE J. Ocean. Eng.*, vol. 26, no. 4, pp. 522–525, Oct. 2001.

[4] Z. Li, D. Li, L. Lin, and Y. Chen, "Design considerations for electromagnetic couplers in contactless power transmission systems for deep-sea applications," *J. Zhejiang Univ. Sci. C*, vol. 11, no. 10, pp. 824–834, 2010.

[5] T. Orekan, P. Zhang, and C. Shih, "Analysis, design, and maximum power-efficiency tracking for undersea wireless power transfer," *IEEE J. Emerg. Sel. Topics Power Electron.*, vol. 6, no. 2, pp. 843–854, Jun. 2018.

[6] J. Shi, D. Li, and C. Yang, "Design and analysis of an underwater inductive coupling power transfer system for autonomous underwater vehicle docking applications," *J. Zhejiang Univ. Sci. C*, vol. 15, no. 1, pp. 51–62, 2014.

[7] T. Kan, R. Mai, P. P. Mercier, and C. C. Mi, "Design and analysis of a three-phase wireless charging system for lightweight autonomous underwater vehicles," *IEEE Trans. Power Electron.*, vol. 33, no. 8, pp. 6622–6632, Aug. 2018.

[8] T. Kan, Y. Zhang, Z. Yan, P. Mercier, and C. C. Mi, "A rotation-resilient wireless charging system for lightweight autonomous underwater vehicles," *IEEE Trans. Veh. Technol.*, vol. 67, no. 8, pp. 6935–6942, Aug. 2018.